Dynamics of probe in network of polymeric cation exchanger studied by Fourier transform analysis of Mössbauer spectra

K. V. Shaitan,[a] M. G. Mikhailyuk,[a]★ A. S. Plachinda,[b] and V. I. Khromov[c]

[a]*Department of Biology, M. V. Lomonosov Moscow State University, Leninskie Gory, 119992 Moscow, Russian Federation. Fax: +7 (095) 939 1115. E-mail: mmax@biophys.msu.ru*
[b]*N. N. Semenov Institute of Chemical Physics, Russian Academy of Sciences, 4 ul. Kosygina, 119991 Moscow, Russian Federation. Fax: +7 (095) 938 2156. E-mail: plachinda@chph.ras.ru*
[c]*D. I. Mendeleev University of Chemical Technology of Russia, 9 Miusskaya pl., 125190 Moscow, Russian Federation. Fax: +7 (095) 200 4204. E-mail: khromov@muctr.edu.ru*

Limited diffusion of the ferric hydroxide (ferrihydrite) nanoparticles in the polymeric network of the AG 50W-X2 sulfonated cation exchanger solvated with aqueous solutions of glycerol (70 and 90 wt.%) was studied in the temperature interval from 90 to 293 K. The Mössbauer spectra were obtained in three windows (250, 25, and 5 mm/s) because of large line broadenings observed in the experiment. The procedure of "seaming" of the time-dependent correlation functions $\langle[\Delta x(t)]^2\rangle$ obtained by the Fourier transform analysis of the initial Mössbauer spectra made it possible to observe the behavior of the function in the extremely wide time range from 0.4 to 360 ns. The observed plateau of the function at long times is a direct proof of the limited nature of the motion. The experimental data were interpreted in the framework of physical models of limited diffusion.

Key words: Mössbauer spectroscopy, Mössbauer probe, ferrihydrite nanoparticles, polymeric cation exchanger, Fourier transform, time-dependent correlation function, limited diffusion.

Mössbauer spectroscopy is a highly efficient tool for studying atomic vibrations, diffusion, and more complicated motions of the type of limited diffusion characteristic of the intramolecular dynamics of proteins and synthetic polymers in the highly mobile state[1—3] and diffusion of atoms and small particles[4—8] "in cage." Analysis of the Mössbauer effect probability and the shape of Mössbauer spectra can provide the displacement value, the diffusion coefficient, the distribution of correlation times, and the potential mode in which the motion occurs.[9—11]

The shape of the Mössbauer spectrum is determined by the Van Hove correlation function,[12] which allows one to find the time-dependent correlation functions of coordinates using the Fourier transform analysis of the Mössbauer spectra.[13] These correlation functions are in fact experimentally determined quantities with independent value even without further processing. At the same time, to choose an adequate physical model, it is sometimes more convenient to deal with time-dependent correlation functions rather than with the initial Mössbauer spectra.

A few experimental works studying the intramolecular dynamics of proteins using the Fourier transform analysis of the Mössbauer spectra are known to date.[14—16] In this work, another system is studied: the solvated polymeric network with moving nanoparticles containing the Mössbauer ^{57}Fe atoms. This allows, first, variation in much wider limits of the values and characteristic times of displacements. Second, the knowledge of the size and weight of a moving object brings an additional certainty to the interpretation of dynamic measurements. In addition, the present work is of interest for the development of the Mössbauer probe method because the parameters of the motion of particle-probes are very sensitive to the specific feature of the supramolecular structure of solvated polymeric ion exchangers, sorbents, and membranes at the spatial level comparable with the size of the probe.

Experimental

The Mössbauer spectra were obtained on a KFKI Mössbauer spectrometer (Hungary) with an NZ-640 motion system, providing the velocity of a source ±150 mm s^{-1}. The Mössbauer source was ^{57}Co(Cr) with an activity of 50 mCi produced at the Physical Energetic Institute (Obninsk).

Published in Russian in *Izvestiya Akademii Nauk. Seriya Khimicheskaya,* No. 12, pp. 2038—2048, December, 2002.

1066-5285/02/5112-2196 $27.00

The AG 50W-X2 polymeric sulfonic cation exchanger (Dowex 50, analytical grade) was chosen for studies. It represents a sulfonated polymeric network with the gel structure based on polystyrene crossed-linked by 2% divinylbenzene. This polymer was chosen because the limited diffusion of the iron hydroxide nanoparticles has previously been found in such networks and studied by Mössbauer spectroscopy. The particles of Fe^{III} hydroxide (ferrihydrite) were precipitated in the matrix of the hydrated cation exchanger with a 10% excess (with respect to the total exchange capacity of the cation exchanger) of a 0.02 *M* solution of NaOH. As shown previously,[6] a nanoparticle in such a solvated cation exchanger is in "cage" formed by the units of a three-dimensional polymeric network and the limited diffusion parameters (diffusion coefficient and maximum displacement) can be varied by changing the temperature, the viscosity of the solvating liquid, or the content of the solvating liquid and the concentration of cross-links in the network. In this work, we studied samples solvated by aqueous solutions of glycerol with a concentration of 90 and 70 wt.% (viscosity of 1.95 and 0.24 P, respectively, at 293 K)[17] in the temperature interval from 90 to 293 K. The solvation was carried out by the replacement of water in the hydrated cation exchanger. The mass fractions of the solvating liquid in the maximally swollen cation exchanger were 85 and 80 wt.% at glycerol concentrations of 70 and 90 wt.%, respectively. The prepared samples were placed in plugged cells, whose weights were monitored during prolonged experiments to prevent changes in the viscosity of the solvating liquid because of the occasional evaporation or sorption of water.

In Mössbauer experiments, the sample thickness with respect to the Mössbauer isotope was chosen in such a way that, on the one hand, the distortion of the lineshape and the effect value are avoided and, on the other hand, a substantially intense spectrum is obtained. In our experiment, the linewidth changed up to 200-fold with temperature. Due to this, the sample optimum in thickness at one temperature became inappropriate for measurements at another temperature. It was insufficient to monitor the thickness by changing the weight of the sample and, therefore, the isotopic composition of iron was also changed, using both natural (the content of the ^{57}Fe isotope was 2.16%) and enriched (96% ^{57}Fe isotope) iron in the synthesis. Therefore, we optimized experiment changing the sample thickness from 0.3 to 12.0 mg of $^{57}Fe\ cm^{-2}$. The measured samples were almost identical (including total concentration of iron in the resin), being different only in the ratio of the iron isotopes and sample weight. The maximally accessible experimental observation window of 250 mm s^{-1} was used to observe very large dynamic broadenings. The central region of the spectrum with the basically important peculiarities could not be detected with the necessary degree of resolution. Therefore, the spectra in narrower windows of 25 and 5 mm s^{-1} were additionally obtained.

Data processing. The procedure of Fourier transform of the Mössbauer spectrum and determination of the time-dependent correlation function is the following. The spectrum in the form of a set of experimental points (G_{exp}) was divided into two components: the smooth background line (G_f) and spectral line $g(w)$

$$G_{exp} = G_f - Sg(w), \qquad (1)$$

where s is the normalization factor. The experimentally determined function (1) was specified at the finite set of channels (or frequencies w). This function is determined by a set of the numbers of pulses $NI(k)$ in each channel "k." The G_f value was found with some experimental error, which increased if the spectral line did not reach saturation within the given experimental window.

The first step in determination of the correlation function $\Phi(t)$ is finding the regularization operator (or the physically justified procedure), which allows generation of the probing functions $\Phi(t)$. In this case, the right part of the equation is determined in the form of a series of N_0 non-negative Lorentzians

$$L'_j(k) = A_j[p_j\Gamma_0/(2\pi)]/[\omega_k^2 + (p_j\Gamma_0/2)^2], \qquad (2)$$

$$i.e.,\ Sg(w) = \sum_j L'_j.$$

The widths of the Lorentzians ($p_j\Gamma_0$) are fixed and form the divergent sequence according to the Müntz theorem.[13] This basically distinguishes the approach used from the formal procedure of approximation of the spectral curve. The $\{A_j\}$ set and the G'_f background parameter are found by minimization of the function

$$G_{exp} - G'_f + \sum_j L'_j = 0. \qquad (3)$$

The surface area (S) above the experimental spectrum, which was determined below the background level G'_f, is the following:

$$S = \sum_j A_j.$$

Let us determine the values

$$\sigma_j = A_j/S = A_j/\sum_j A_j,$$

which represent the normalized contribution of the jth Lorentzian

$$(\sum_j \sigma_j = 1).$$

Using Eqs. (1) and (3) and the known formula for the Fourier transform of the Lorentzian, we obtain the Van Hove correlation function $\Phi(t) = \langle \exp(ix(0)/\lambda)\exp(-ix(t)/\lambda)\rangle$ in the following form:

$$\Phi(t,\{p_j\}) = \sum_{j=1}^{N_0} \sigma_j \exp(-p_j\Gamma_0 t/2).$$

This procedure determines, in fact, the regularization operator, which is used for the generation of probing functions. The optimum series (p_j) was chosen from requirements of maximum smoothness $R(t) = \Phi(t,\{p_j\})$, which is virtually performed by minimization of the stabilizing functional

$$\Omega(R) = \int_0^\infty [(dR/dt)^2 + R^2]dt.$$

Then the correlation is used

$$\Omega(R) = \sum_i^{N_0}\sum_j^{N_0} \sigma_i\sigma_j(1 + p_i p_j)/(p_i + p_j).$$

Our studies showed that the most appropriate was the power series $\{p_j\}$ with the base 2

$$p_j = (1 + 2^{j-m}), \quad (4)$$

where j is the number of the Lorentzian ($1 \le j \le M_0$), and m is the parameter increasing the number of terms in the series under the condition

$$\Gamma_0 2^{M_0-m} < N_k \Delta\omega_k.$$

Due to the general properties of the Fourier transform, we obtain the $\Phi(t)$ function in the time interval

$$t = [(N_k\Delta\omega_k/4)^{-1}, (2\Delta\omega_k)^{-1}],$$

where $\Delta\omega_k$ is the value of a channel, and N_k is the total number of channels. Both the natural width and the dynamics of the Mössbauer nucleus contribute to the width of the Mössbauer spectrum. Therefore, an information about the behavior of the correlation function is in the difference between the spectra in the presence and absence of dynamic broadenings, due to which the behavior of the correlation function at the time $t \gg \Gamma_0^{-1}$ cannot be investigated in principle.

More rigorous treatment requires a correct solution of the problem on errors in determination of $\Phi(t)$ taking into account statistical errors of the transformed spectra and the minimum width of the observation window, because at the window width $N_k\Delta\omega_k < \Gamma_0/2$ the spectrum becomes less informative. Based of our studies[18] of the Fourier transform of the Mössbauer spectra with different signal/noise ratios and their recovery from the time correlation functions, we can estimate the time intervals of reliable observation of the correlation functions

$$\begin{aligned} t &\in [(N_k\Delta\omega_k/4)^{-1}, (2\Delta\omega_k)^{-1}] \text{ at } \Delta\omega_k > \Gamma_0/2, \\ t &\in [(N_k\Delta\omega_k/4)^{-1}, (10\Delta\omega_k)^{-1}] \text{ at } \Delta\omega_k \approx \Gamma_0/2, \\ t &\in [(N_k\Delta\omega_k/4)^{-1}, (\Gamma_0/2)^{-1}] \text{ at } \Delta\omega_k \le \Gamma_0/10, \end{aligned} \quad (5)$$

where Γ_0 is the natural width of the Mössbauer line.

Thus, the right edge of the time interval is restricted by the Γ_0 value. The left edge is determined by the width of the experimental observation window. Therefore, its displacement toward shorter times is limited only by experimental possibilities of the instrument.

It was also established that the relative error of determination of the Van Hove autocorrelation function and, correspondingly, the time dependence of the mean square probe displacement in the framework of this method does not exceed the statistical error for the experimental measurements of the Mössbauer spectrum.

The line of any experimental Mössbauer spectrum is known to be broadened (in addition to the natural width Γ_0) due to the individual properties of the absorber and source, the final thickness of the absorber, and apparatus effects. Therefore, the correct Fourier transform procedure needs to take into account not only the natural linewidth Γ_0 but also the lineshape in the experimental spectrum of this substance in the absence of dynamic broadenings.

The correlation function will be determined in the form $\Phi(t,Y) = R(t,Y)/R(t,Y_0)$, where $R(t,Y_0)$ is the regularizing operator for the initial Mössbauer spectrum in the absence of dynamic broadenings, and Y is the parameter changing the state of the system. In our case, the state of the system under study changes with the temperature change, *i.e.*, $Y_0 = T_0 = 100$ K (dynamic broadenings are absent), and $R(t,Y) = R(t,T)$ is the operator for the dynamically broadened spectrum at the temperature T.

In this work we observed very large dynamic broadenings, which exceeded the width of the initial spectral line by three orders of magnitude in the limit. The detection of the initial Mössbauer spectra in windows with different widths make it possible to determine the correlation function in the widest time interval, *viz.*, from the shortest (the spectrum measured in the broadest window) to the longest times (the part of the total spectrum measured in the narrowest window). In the general case, the correlation function is determined with an accuracy to some additive constant, whose value depends on the ratio of the surface area of the experimental spectrum, which subjected to Fourier transform in a specific observation window, to its total surface area. This constant is equal to zero only when the whole spectrum is completely within the observation window. Under real conditions, one has to "seam" correlation functions corresponding to the spectra in different observation windows. The procedure of "seaming" is the following. The correlation function measured in the widest observation window is "seamed" to the function obtained from the spectrum measured in a narrower window. With this purpose, some time-independent constant should be added to the function corresponding to the spectrum in a narrower window. This constant is determined in such a way that the divergence between the seamed functions in the region of their overlap would be minimized. The "seaming" of correlation functions is equivalent to such a procedure of obtaining the spectrum as if the spectrum, which is more informative with respect to longer times, *e.g.*, obtained in a narrower window (25 mm s^{-1}) and with a much less value of channel $\Delta\omega_k$, would be inserted into the central part of the Mössbauer spectrum obtained, *e.g.*, in a wide window (250 mm s^{-1}).

The relation of the mean square of the displacement of probe particles $\langle[\Delta x(t)]^2\rangle$ can be normalized by two methods. In the first case, the $\langle x^2\rangle$ value determined from the numerical values of the fraction of the elastic component in the spectra is the limiting value at $t \gg \tau_c$ (τ_c is the relaxation (correlation) time of motions). In the case of limited diffusion, the mean square of the displacement of probe particles at $t \gg \tau_c$ tends to its limiting value, and the spectral function remains normalized to unity

$$\int_{-\infty}^{+\infty} g(\omega)\mathrm{d}\omega = 1.$$

However, the processed Mössbauer spectra contain information on the behavior of the correlation function in the restricted time interval determined by formula (5). If the correlation time is of an order of the lifetime of the Mössbauer level in the excited state, then the spectra measured in the maximally accessible observation window should be used to find the limiting $\langle[\Delta x(t)]^2\rangle$ values. The procedure of "seaming" allows the $\langle[\Delta x(t)]^2\rangle$ time functions to lock to the ordinate with a good accuracy. In this work we consider such large dynamic broadenings that for the maximum observation window, when the value of a channel becomes higher than the Γ_0 linewidth, the elastic component of this spectrum is very poorly resolved. In this case, normalization of the time function along the ordinate axis by its extrapolation to zero at $t = 0$ becomes insufficient. Therefore, for the final

normalization of the seamed function along the ordinate, we used the numerical $\langle x^2 \rangle$ value obtained from the Mössbauer effect probability

$$f^{\prime} = \exp(-\langle x^2 \rangle / \lambda^2), \quad (6)$$

which is determined in the direct Mössbauer experiment in the window optimum for this task. For very high rates of limited diffusion when only the non-broadened (elastic) spectral component remains within the limit in the observation window, the direct determination of the Mössbauer effect probability $f^{\prime}$ remains to be the only method for determination of the $\langle x^2 \rangle$ value, which is independent of t, in this case, in the limits accessible for observation.

Results and Discussion

The probe substance in the studied samples was Fe^{III} hydroxide (ferrihydrite). According to the published data,[19—21] including the electron microscopic studies, primary ferrihydrite particles ~3 nm in diameter are formed under the used conditions of precipitation. Studies with Mössbauer spectroscopy at 4.2 K showed the presence of ferrihydrite in the cation exchanger. The temperature of transition from the antiferromagnetic to superparamagnetic state ("blocking temperature") T_B = 15 K corresponded to the particle diameter of ~3 nm.

In this work, the Mössbauer spectra of the dry and solvated samples were obtained in the temperature interval from 90 to 300 K. The spectrum of the dry sample in this temperature interval also corresponds to ferrihydrite and is a quadrupole doublet. The large linewidth (Γ = 0.49 mm s^{-1}) and weak asymmetry of this doublet are explained by some distribution of the quadrupole splitting and isomeric shift values due to the nonequivalent positions of iron in the ferrihydrite structure. This broadening is virtually constant in the 77—300 K interval to confirm unambiguously that it is caused by the structure rather than dynamics. Thus, the spectra of the dry sample have no dynamic broadening up to T = 300 K. The Mössbauer effect probability for the particles studied and its temperature dependence are close to those for bulky iron hydroxide, and the mean square displacements calculated from the temperature plot depend linearly on the temperature according to the Einstein and Debye models. Therefore, the dynamics of the probe particles, which are densely compressed in the glassy cation exchanger matrix, is presented by vibrations of iron atoms inside the particles rather than motions of the particles as a whole. Therefore, this spectrum was accepted as initial to be used in the Fourier transform procedure.

The pattern changes drastically for the solvated samples. Due to swelling of the polymeric network during solvation, particles occur in "cages" with the liquid. At T < 200 K this matrix is glassy. The spectrum of the particles incorporated in this matrix and the Mössbauer effect probability in this temperature interval do not differ from those for the dry sample. However, beginning from 200 K (the sample with a solution of glycerol in a concentration of 70 wt.%) and 250 K (the sample with a solution of glycerol in a concentration of 90 wt.%), broadenings reaching very high values at higher temperatures appear in the spectra of the solvated samples (Figs. 1—4). As a result, the spectrum gains a characteristic shape of superposition of the elastic (non-broadened) and quasielastic (broadened) components, directly indicating the limited diffusion of the particles.

The motion of particles begins to manifest itself in the Mössbauer spectrum in the region of temperatures of the solvate devitrification. The further increase in the intensity of motions is associated with both the temperature increase and decrease in the liquid viscosity. However, one more circumstance should be considered. It has previously been shown by Mössbauer spectroscopy,[2] Rayleigh scattering of Mössbauer radiation,[22] and slow neutron scattering[23] that the polymeric networks of cation exchanger (including the styrenedivinylbenzene cation exchanger studied in this work) transfer to the mobile state under their solvation at room temperature. The authors of the same works observed the transition to the mobile state of solvated cation exchangers, which were frozen in liquid nitrogen, with the temperature increase above the temperatures of devitrification or melting of the solvate. Thus, in our case, we deal with the motion of a particle in the "cage with moving walls." The question arises about the interrelation of these motions. In other words, whether the probe particles follow the polymeric network or they move quasi-independently? For the polystyrenedivinylbenzene cation exchanger network (labeled with the $^{57}Fe^{3+}$ ions), transition to the mobile state is expressed as a decrease in the Mössbauer effect probability by approximately an order of magnitude. However, this does not result in broadenings in the Mössbauer spectrum, and changes are observed in a much higher-frequency region, namely, in the slow neutron scattering spectra. Thus, the solvation of this dry cation exchange is accompanied by an increase in the mobility of the polymeric network only in the high-frequency region, and it is not manifested in the Mössbauer spectrum shape. Therefore, the slower and with greater displacements motions of the probe particles observed by us do not repeat the displacements of the network.

The overdamped Brownian oscillator model[9,24] is most popular for the description of Mössbauer spectra in the presence of limited diffusion. In this case, the lineshape of the spectrum is given by the expression

$$I(\omega) \approx \left(\frac{-k^2 D}{d}\right) \sum_{n=0}^{\infty} \left(\frac{-k^2 D}{d}\right)^n \frac{1}{n!} \left[\frac{(\Gamma_0/2 + nd)}{(\omega - \omega_0)^2 + (\Gamma_0/2 + nd)^2}\right], \quad (7)$$

where D is the diffusion coefficient, d is the ratio of the elastic to friction coefficients, and $k = 2\pi/\lambda$ is the wave

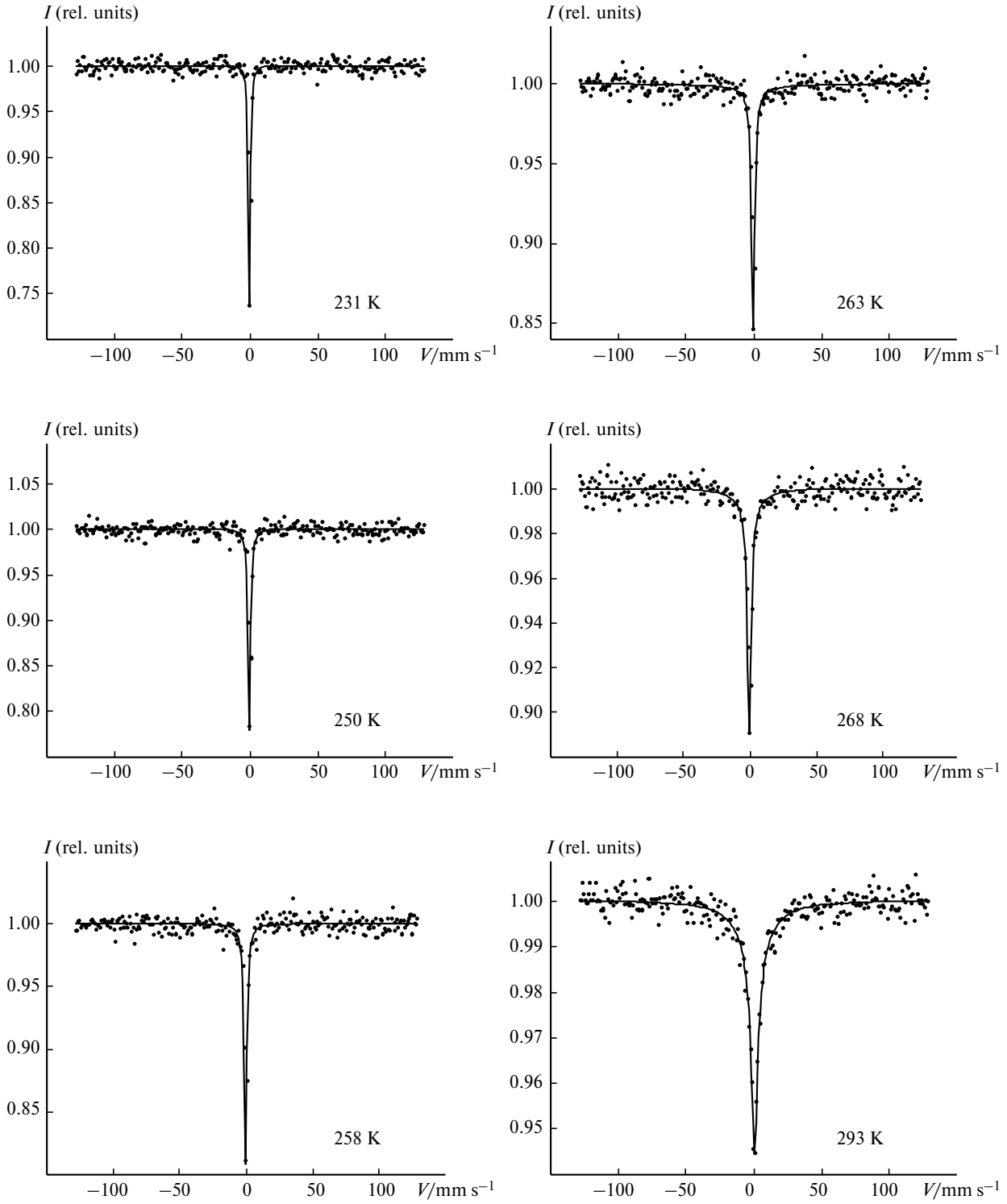

Fig. 1. Temperature series of the Mössbauer spectra for the cation exchanger solvated by an aqueous solution of glycerol (90 wt.%), in an observation window of 250 mm s^{-1}. Points are experiment, and solid lines are the result of processing by a series of non-negative Lorentzians (in all cases, the dispersion value $d < 0.01$).

number (λ = 0.86 Å for ^{57}Fe). It has earlier[9,11] been shown that another model is preferable for the description of the temperature dependence of the motion of particles in the cage, namely, the model of continuous diffusion in

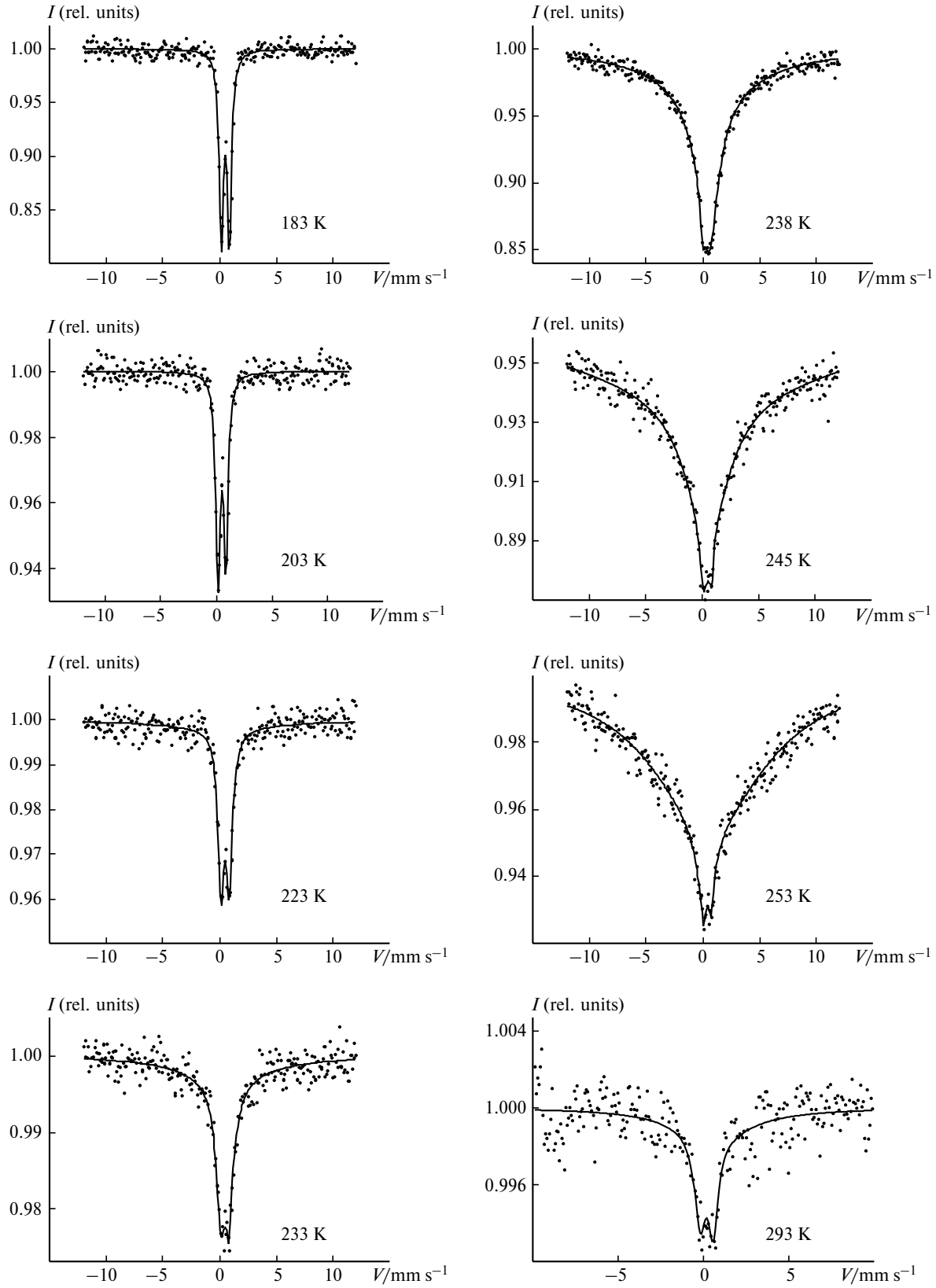

Fig. 2. Temperature series of the Mössbauer spectra for the cation exchanger solvated by an aqueous solution of glycerol (70 wt.%) in an observation window of 25 mm s^{-1}. Points are experiment, and solid lines are the result of processing by a series of non-negative Lorentzians (in all cases, the dispersion value $d < 0.01$).

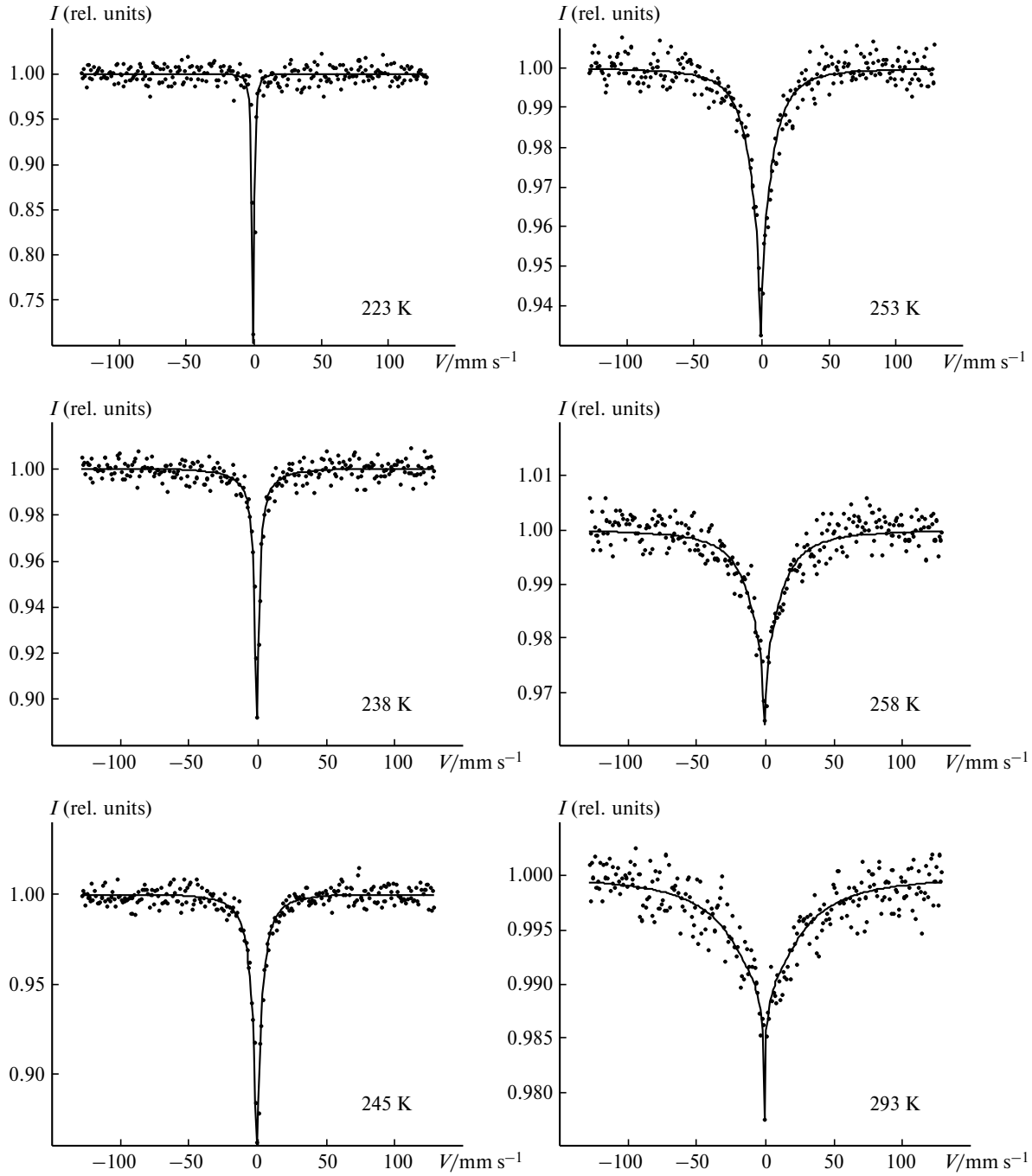

Fig. 3. Temperature series of the Mössbauer spectra for the cation exchanger solvated by an aqueous solution of glycerol (70 wt.%) in an observation window of 250 mm s^{-1}. Points are experiment, and solid lines are the result of processing by a series of non-negative Lorentzians (in all cases, the dispersion value $d < 0.01$).

the rectangular potential, resulting in the following spectral shape:

$$I(\omega) \approx \frac{A_{00}\Gamma_0/2}{(\omega-\omega_0)^2+(\Gamma_0/2)^2} + \sum_{l=0}^{\infty}\sum_{n=0}^{\infty}\frac{(2l+1)A_{ln}(\Gamma_0/2+D\lambda_{ln})}{(\omega-\omega_0)^2+(\Gamma_0/2+D\lambda_{ln})^2}, \quad (8)$$

where $A_{ln} = \frac{6\mu_{ln}^2}{\mu_{ln}^2 - l(l+1)}\left[\frac{kaj_{j+1}(ka) - lj_l(ka)}{(ka)^2-\mu_{ln}^2}\right]^2$

at $l, n \neq 0$,

$$A_{00} = 9[\sin(ka) - ka\cos(ka)]^2/(ka)]^2,\ \lambda_{ln} = (\mu_{ln}/a)^2,$$

μ_{ln} is the nth root of the transcendent equation $j'_l(\mu) = 0$, a is the radius of the spherical cavity formed by the poten-

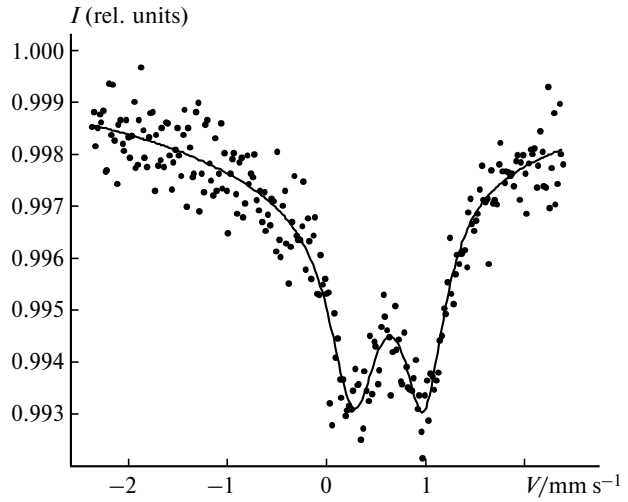

Fig. 4. Mössbauer spectrum of the cation exchanger solvated with an aqueous solution of glycerol (70 wt.%) in an observation window of 5 mm s^{-1} at $T = 293$ K. Points are experiment, and solid lines are the result of processing by a series of non-negative Lorentzians (in all cases the dispersion value $d < 0.01$).

tial well, and $j_l(Z) = Z^l(-Z^{-1}d/dZ)^l(\sin Z/Z)$ is the spherical Bessel function.

The spectra obtained by us (see Figs. 1—4) are satisfactorily described by both formulas. Using both models, we determined the numerical coefficients of limited diffusion (Tables 1 and 2). The formal approximation of the Mössbauer spectra by the set of Lorentzian curves and extraction of the fraction of the elastic component in the spectra allow one to find the Debye—Waller factor f' (6) and the corresponding values of displacements of the probe particles (see Tables 1 and 2).

Let us compare the obtained plots of the mean square of the probe displacement *vs.* time, which are experimental functions, with the specific model plots $\Phi(t)$ and let us determine the numerical values of the parameters of the model. In the overdamped Brownian oscillator model,[25] these plots are described by the formula

$$<[x(t) - x(0)]^2> = 2A^2[1 - \exp(-t/\tau_c)], \qquad (9)$$

where A^2 is the root-mean-square amplitude of vibrations, $\tau_c = \gamma/M\omega_0^2$, ω_0 is the frequency of free vibrations of the oscillator, and M is the weight of the probe. The γ coefficient is related to the microviscosity of the system η by the Stokes—Einstein correlation $\gamma \approx 6\pi r\eta$, where r is the characteristic radius of the probe. The γ coefficient can be recalculated to the diffusion coefficient $D = kT/\gamma$.

These plots were processed using the formula

$$<[\Delta x(t)]^2> = 2A_1^2[1 - \exp(-t/\tau_1)] + 2A_2^2[1 - \exp(-t/\tau_2)]. \qquad (10)$$

In formula (10) the $<[\Delta x(t)]^2>$ plot is described by the sum of terms responsible for the displacement of the probe, and the contribution to the dynamics of different components of the motion can also be redistributed with temperature. These terms are responsible for the fast and slow degrees of freedom. Figure 5 represents the case when the processing of the experimental plot using formula (9) containing one Brownian oscillator gives a greater error than the processing using Eq. (10).

The obtained plots of the mean square displacement of the probe particles $<[\Delta x(t)]^2>$ are presented in Figs. 6—8. Tables 1 and 2 contain the results of processing of the plots presented in Figs. 7 and 8, respectively. Figure 9 illustrates the procedure of "seaming" (see Fig. 7): the $<[\Delta x(t)]^2>$ functions obtained by the processing of the Mössbauer spectra detected at the same temperature but in different observation windows are presented in the same plot.

As can be seen in Table 1, for the cation exchanger solvated by a 70% solution of glycerol, the total amplitude of displacement of the probe particles increases from 0.03

Table 1. Parameters of the limited diffusion of the probe* in the cation exchanger (70% solution of glycerol) in the time interval t = [0.4 ns; 71 ns]

T/K	A_1	A_2	τ_1	τ_2	D/cm^2 s^{-1}
	Å		ns		
203	0.03	—	14.8	—	—
223	0.09	—	48.3	—	$1 \cdot 10^{-10}$
233	0.12	—	23.1	—	$4 \cdot 10^{-10}$
238	0.1	0.18	4.5	90.9	$1 \cdot 10^{-9}$
245	0.12	0.15	6.2	29	$1.7 \cdot 10^{-9}$
253	0.15	0.14	3.1	31.9	$5 \cdot 10^{-9}$
293**	0.19	0.09	1.7	42.8	$1.4 \cdot 10^{-8}$

* The A and τ values were obtained by processing of the experimental correlation function in the Brownian oscillator model (using formulas (9) and (10)), and the diffusion coefficient D was obtained by the direct processing of the initial Mössbauer spectra in the Brownian oscillator model (using Eq. (7)).
** The time interval is t = [0.4 ns; 360 ns].

Table 2. Parameters of the limited diffusion of the probe* in the cation exchanger (90% solution of glycerol) in the time interval t = [0.4 ns; 71 ns]

T/K	A/Å	τ/ns	D/cm^2 s^{-1}
231	0.04	156	$6 \cdot 10^{-11}$
250	0.08	28.7	$1.7 \cdot 10^{-10}$
258	0.07	9.5	$2.5 \cdot 10^{-10}$
263	0.08	2.2	$3.5 \cdot 10^{-10}$
268	0.09	3.0	$6 \cdot 10^{-10}$
293	0.14	2.9	$2 \cdot 10^{-9}$

* The A and τ values were obtained by processing of the experimental correlation function in the Brownian oscillator model (using formula (9)), and the diffusion coefficient D was obtained by the direct processing of the initial Mössbauer spectra in the Brownian oscillator model (using Eq. (7)).

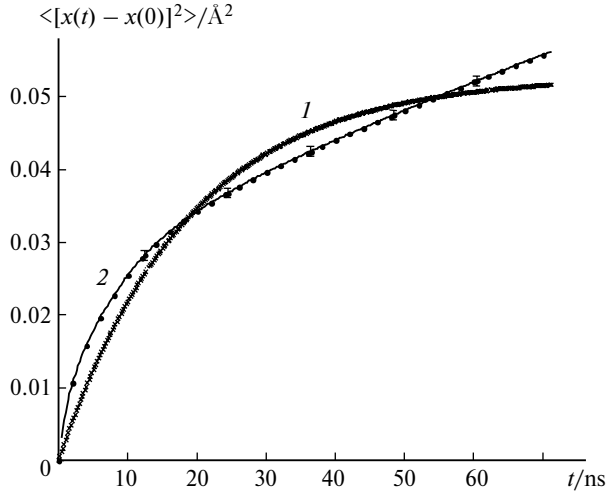

Fig. 5. Mean square displacement of the probe as a function of time for the cation exchanger solvated with an aqueous solution of glycerol (70 wt.%) at $T = 238$ K: the experimental data (points) and the result of processing using the Brownian oscillator model by formulas (9) (curve *1*) and (10) (curve *2*).

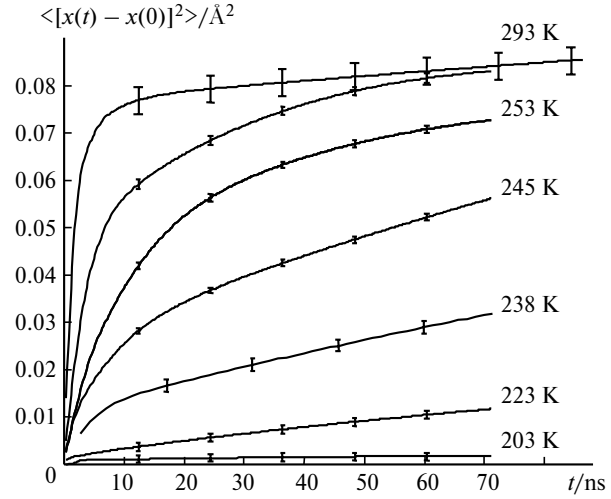

Fig. 7. Mean square displacement of the probe as a function of time obtained by the procedure of "seaming" for two temperature series of the cation exchanger samples measured in windows of 250 and 25 mm s^{-1} (70% solution of glycerol). The confidence interval is indicated for each curve.

to 0.28 Å with the temperature increase from 203 to 293 K. The correlation times for the relatively fast motions decrease by an order of magnitude and reach ~1.7 ns at 293 K. At 293 K the time plot of the mean square of the probe displacement virtually achieves its limiting values already during the observed time interval (see Fig. 7). The $<[\Delta x(t)]^2>$ plot, which was obtained from the Mössbauer spectrum in a minimum observation window of 5 mm s^{-1}, at the same temperature reaches the limit at the times >100 ns (Fig. 10). This is a direct evidence for the limited nature of diffusion.

It follows from Table 2 that, in the case of the cation exchanger solvated with a 90% solution of glycerol, three

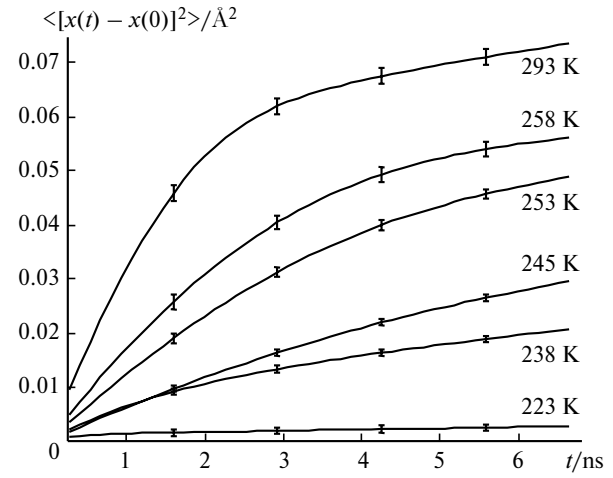

Fig. 6. Mean square displacement of the probe as a function of time for the cation exchanger solvated with an aqueous solution of glycerol (70 wt.%) in an observation window of 250 mm s^{-1}. The confidence interval is indicated for each curve.

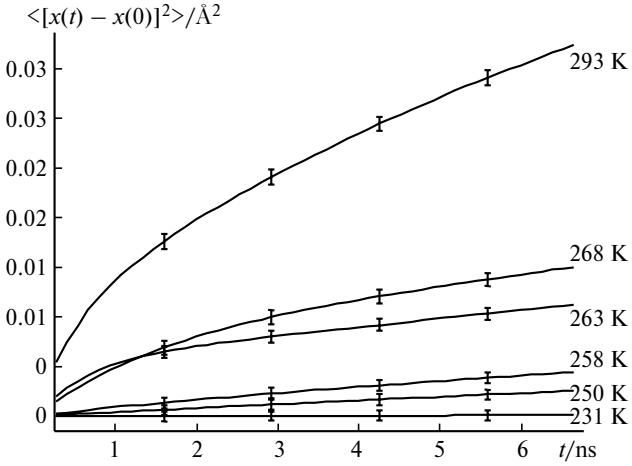

Fig. 8. Mean square of the displacement of the probe as a function of time for the cation exchanger solvated with an aqueous solution of glycerol (90 wt.%) in an observation window of 250 mm s^{-1}. The confidence interval is indicated for each curve.

noticeable jumps are observed in the temperature interval from 231 to 293 K. They appear as an approximately twofold increase in the amplitude of displacement of the iron hydroxide particles near 240, 260, and 270 K. The characteristic correlation times decrease sharply at the same temperatures. Perhaps, this is explained by the nonuniform distribution of the devitrification temperatures of the solvate, and the correlation time is a parameter characterizing the structure nonuniformity.

It has already been indicated that at low temperatures ($T < 200$ K) the spectra of the dry and solvated samples are the same. The Mössbauer effect probability for them is determined only by vibrations of the Fe atoms inside the

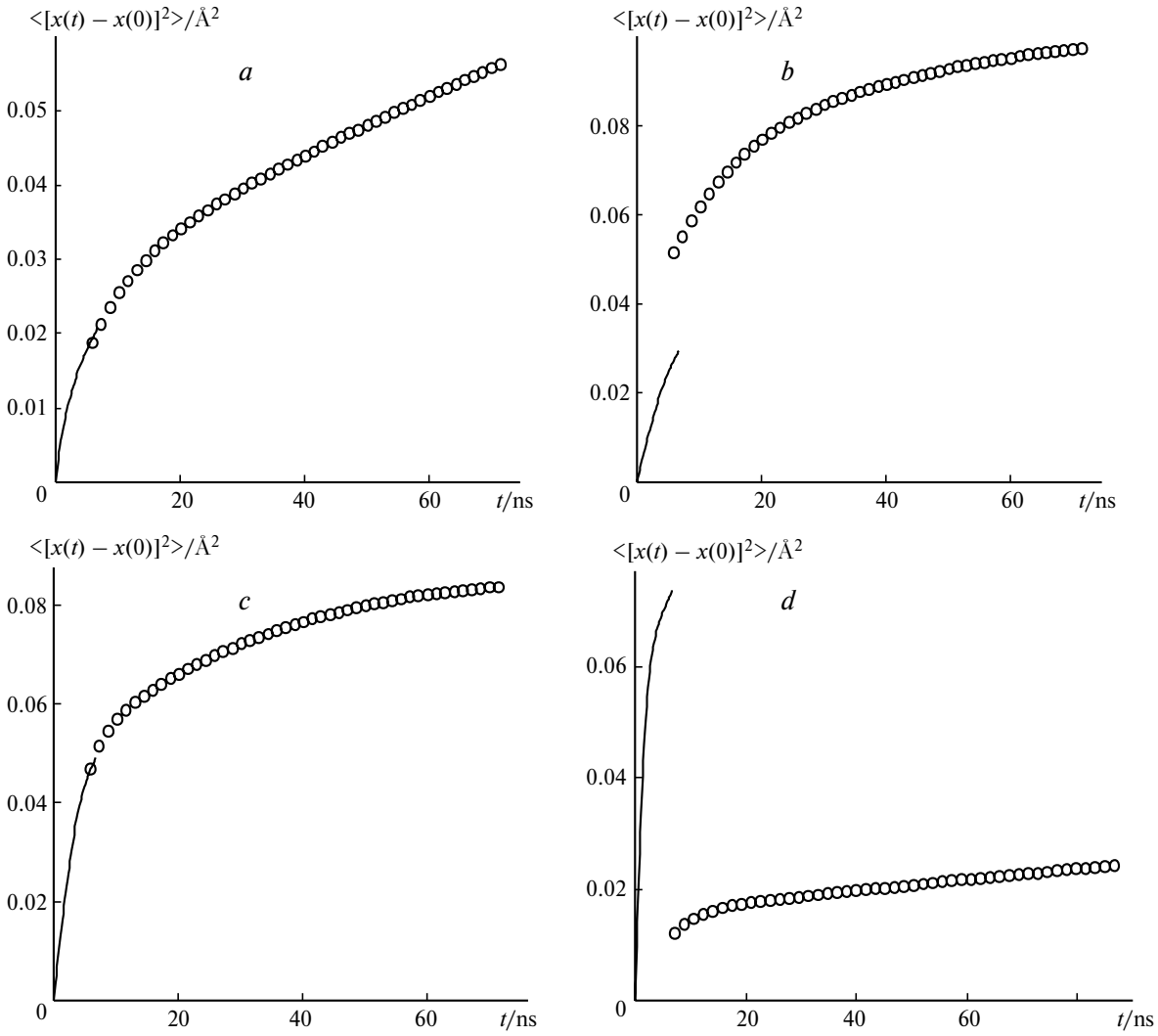

Fig. 9. Example of the time function of the mean square of probe displacement for two temperature series of the cation exchanger (a 70% solution of glycerol) measured in windows of 250 mm s^{-1} (solid lines) and 25 mm s^{-1} (circles) at the temperatures 238 (*a*), 245 (*b*), 253 (*c*), and 293 K (*d*).

probe particles. The value of these displacements of the atoms is $\langle x^2\rangle_{at} = 0.0042$ Å^2 at 80 K and increases for the dry sample to $\langle x^2\rangle_{at} = 0.0155$ Å^2 at 293 K. For the cation exchanger solvated by a 90% solution of glycerol, after the appearance of dynamic broadenings in the spectrum at $T = 250$ K, the total surface area of the spectrum, including the elastic and quasielastic components, changes with the further temperature increase in the same way as that for the dry sample. This implies that the atomic vibrations of the iron particles and their temperature dependence are the same in the dry and solvated samples. As a result, the dynamics of the probe in this sample at 293 K is completely described by two components: (1) motion of the particle as a whole with $\langle x^2\rangle_{part}$ and its time dependence (see Fig. 8) and (2) intraparticle atomic vibrations with $\langle x^2\rangle_{at} = 0.0155$ Å^2. In this case, $\langle x^2\rangle_{part}$ at $t = 6$ ns does not reach saturation.

The situation is different for the more mobile sample solvated by a 70% solution of glycerol. With the temperature increase, beginning from 245 K, the spectral line does not already reach saturation even in the maximum window of 250 mm s^{-1}. However, this is satisfactorily described by both models: the Brownian oscillator and the rectangular potential well. However, at the temperature higher than 253 K, the total model area of the Mössbauer spectrum additionally decreases and reaches $f' \approx 0.3$ at 293 K, *i.e.*, only 1/3 of the total area of the spectrum corresponding to this temperature remains in the maximum window. This means that an additional high-frequency component ($\omega > 1 \cdot 10^9$ s^{-1}) appears in the probe motion. Thus, unlike the less mobile sample (a 90% solution of glycerol), the dynamics of the probe of the highly mobile sample at 293 K is completely described by three components: (1) the intramolecular atomic vibra-

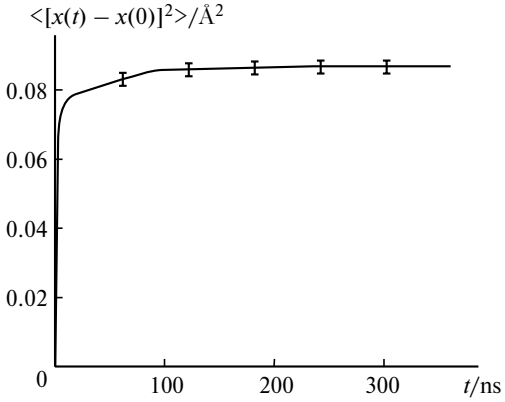

Fig. 10. Result of the "seaming" procedure for the time plots of the mean square of the probe displacement obtained by the Fourier transform of three Mössbauer spectra (T = 293 K) for the cation exchanger measured in windows of 250, 25, and 5 mm s^{-1} (a 70% solution of glycerol). The confidence interval is indicated for each curve.

tions with $\langle x^2\rangle_{at}$ = 0.0155 Å^2, (2) the low-frequency ($1 \cdot 10^6$ $s^{-1} < \omega < 1 \cdot 10^9$ s^{-1}) motions of the particle as a whole of the limited diffusion type with the limiting value $\langle x^2\rangle_{lf}$ = 0.085 Å^2 and its time dependence (see Figs. 6, 7, and 10), and (3) the high-frequency ($\omega > 1 \cdot 10^9$ s^{-1}) motions of the particle as a whole with $\langle x^2\rangle_{hf}' \approx 0.02$ Å^2.

If the low-frequency motions of the particle are completely manifested in the Mössbauer spectrum shape and in the time dependence of the mean square of the probe displacement obtained from the spectrum, then the high-frequency motions are so fast that appear only as a decrease in the total observed Mössbauer effect probability. The mere fact of observation of such motions for the relatively large (~30 Å) and massive (~15000 a.u.) object is of substantial interest.

Thus, we studied the system in which the parameters of the probe motion of the type of limited diffusion vary in very wide limits (diffusion coefficient $D = 6 \cdot 10^{-11}$—$1.4 \cdot 10^{-8}$ cm^2 s^{-1}, amplitude of displacement of the probe particles A = 0.03—0.28 Å), while the procedure of "seaming" of the time-dependent correlation functions using the Fourier transform of Mössbauer spectra made it possible to obtain for the first time the $\langle[\Delta x(t)]^2\rangle$ function in the time interval t = 0.4—360 ns.

This work was financially supported by the Russian Foundation for Basic Research (Project Nos. 01-04-49302 and 00-03-32267), the Ministry of Industry, Science, and Technologies of the Russian Federation, and the Government of Moscow (Grants of Moscow of 2001 Nos. 1.1.144 and 1.2.45).

References

1. I. Chang, H. Hartmann, Yu. Krupyanskii, A. Zharicov, and F. Parak, *Chem. Phys.*, 1996, **212**, 221.
2. A. S. Plachinda, B. N. Laskorin, D. B. Poblinkov, E. F. Makarov, N. G. Zhukova, V. V. Krylova, I. A. Logvinenko, A. Yu. Permogorov, and V. I. Khromov, *Dokl. Akad. Nauk SSSR*, 1985, **280**, 938 [*Dokl. Phys. Chem.*, 1985, **280** (Engl. Transl.)].
3. Yu. F. Krupyanskii, K. V. Shaitan, V. I. Gol´danskii, I. V. Kurinov, A. B. Rubin, and I. P. Suzdalev, *Biofizika*, 1987, **32**, 761 [*Biophysics*, 1987, **32** (Engl. Transl.)].
4. M. A. Krivoglaz and S. P. Repetskii, *Fiz. Tverd. Tela*, 1966, **8**, 2908 [*Sov. Phys. Sol. State*, 1967, **8** (Engl. Transl.)].
5. G. U. Nienhaus and F. Parak, *Hyperfine Interactions*, 1994, **90**, 243.
6. A. S. Plachinda, V. E. Sedov, V. I. Khromov, L. V. Bashkeev, and I. P. Suzdalev, *Chem. Phys. Lett.*, 1990, **175**, 101.
7. A. M. Afanas´ev, L. V. Bashkeev, A. S. Plachinda, V. E. Sedov, and V. I. Khromov, *Khim. Fiz.*, 1989, **8**, 986 [*Chem. Phys. Reports*, 1990, **8** (Engl. Transl.)].
8. A. S. Plachinda, V. E. Sedov, V. I. Khromov, L. V. Bashkeev, and I. P. Suzdalev, *Hyperfine Interactions*, 1990, **56**, 1483.
9. A. M. Afanas´ev and V. E. Sedov, *Phys. Stat. Sol.* (*b*), 1985, **131**, 299.
10. Yu. F. Krupyanskii, V. I. Goldanskii, G. U. Nienhaus, and F. Parak, *Hyperfine Interactions*, 1990, **53**, 59.
11. A. S. Plachinda, V. E. Sedov, V. I. Khromov, I. P. Suzdalev, V. I. Goldanskii, G. U. Nienhaus, and F. Parak, *Phys. Rev.*, *B*, 1992, **45**, 7716.
12. K. S. Singwi and A. Sjolander, *Phys. Rev.*, 1960, **120**, 1093.
13. S. K. Basovets, I. V. Uporov, K. V. Shaitan, Yu. F. Krupyanskii, I. V. Kurinov, I. P. Suzdalev, A. B. Rubin, and V. I. Goldanskii, *Hyperfine Interactions*, 1988, **39**, 369.
14. S. K. Basovets, I. V. Uporov, K. V. Shaitan, Yu. F. Krupyanskii, V. Ya. Rochev, and I. P. Suzdalev, *Khim. Fiz.*, 1989, **8**, 694 [*Chem. Phys. Reports*, 1990, **8** (Engl. Transl.)].
15. I. V. Uporov, S. K. Basovets, K. V. Shaitan, E. F. Makarov, and V. Ya. Rochev, *Khim. Fiz.*, 1990, **9**, 21 [*Chem. Phys. Reports*, 1991, **9** (Engl. Transl.)].
16. V. I. Khromov, A. S. Plachinda, S. I. Kamyshanskii, and I. P. Suzdalev, *Izv. Akad. Nauk*, *Ser. Khim.*, 1996, 886 [*Russ. Chem. Bull.*, 1996, **45**, 841 (Engl. Transl.)].
17. I. Timmermans, *The Physico-Chemical Constants of Binary Systems in Concentrated Solutions*, Int. Publ., New York, 1960, **4**, 309.
18. K. V. Shaitan and M. G. Mikhailyuk, *Khim. Fiz.*, 2001, **20**, 3 [*Chem. Phys. Reports*, 2002, **20** (Engl. Transl.)].
19. J. Dousma and P. L. de Bruyn, *J. Colloid Interface Sci.*, 1978, **64**, 154.
20. J. M. D. Coey and P. W. Readman, *Earth Planet Sci. Lett.*, 1973, **21**, 45.
21. K. J. Atkinson, A. M. Posner, and J. P. Quirk, *J. Inorg. Nucl. Chem.*, 1968, **30**, 2371.
22. A. S. Plachinda, I. P. Suzdalev, I. A. Kuznetsov, Yu. V. Baldokhin, and V. I. Khromov, *Izv. Akad. Nauk*, *Ser. Khim.*, 1998, 1969 [*Russ. Chem. Bull.*, 1996, **47**, 1914 (Engl. Transl.)].
23. A. A. Tumanov, Yu. Yu. Glazkov, and A. V. Abramov, *Otchet* [*Report*], Physical Energetic Institute, Obninsk, 1986, 105 pp. (in Russian).
24. I. Nowik, E. R. Bauminger, S. G. Cohen, and S. Ofer, *Phys. Rev. A*, 1985, **31**, 2291.
25. K. V. Shaitan and A. B. Rubin, *Biophysics*, 1980, **25**, 796.

Received November 16, 2001;
in revised form May 7, 2002